BioNanoScience
https://doi.org/10.1007/s12668-024-01454-5

RESEARCH

Inhibition of EGFR1 in Triple Negative Breast Cancer Cells Using siRNA Loaded with Fe_3O_4 Magnetic Nanoparticles

Javad Parnian[1] · Leila Ma'mani[2] · Mohamad Reza Bakhtiari[1] · Maliheh Safavi[1]

Accepted: 14 May 2024

Abstract
Triple-negative breast cancer (TNBC) is known as the most common cancer among women in the world. Although overexpression of the EGFR1 gene is observed in more than 70% of patients, medications based on inhibitors of this receptor are ineffective. This is due to the fact that the protein remains active, even after administration with inhibitory drugs. We used siRNA to silence the EGFR1 gene in this study. The siRNA was packaged in a magnetic nanoparticle (MNP) that was functionalized with poly ethyleneimine (PEI), PEGylated folic acid (FA-PEG), and β-cyclodextrin (βCD). Multi-functionalized FA-PEG/βCD functionalized PEI-coated iron oxide magnetic nanoparticles (Fe_3O_4@CD-PEI/FA-PEG) were produced by post-surface modification. This multi-functionalized magnetic nanocarrier was structurally verified using scanning electron microscopy (SEM), transmission electron microscopy (TEM), dynamic light scattering (DLS), atomic force microscopy (AFM), and vibrating sample magnetometry (VSM). Small interfering RNAs (siRNA) were used as a precise tool in gene therapy in this study to remove EGFR1 gene mRNA. siRNA molecules are about 21 nucleotides that cause cleavage in the complementary sequence of the target mRNA. The capacity to deliver siRNAs against EGFR1 to the breast cancer cell line (MD-MBA-231) was evaluated. According to flow cytometry, siRNA was efficiently delivered to the cells, with an absorption rate of 62%. In addition, confocal microscopy confirmed the cell uptake and endosomal escape. Also, the expression level of the EGFR1 gene was measured by the quantitative PCR method, which showed a 78% knockdown of this gene at the mRNA level.

Keywords Breast cancer · Magnetic nanoparticles · siRNA · β-cyclodextrin functionalized PEI

1 Introduction

Breast cancer is one of the most common malignancies in women, with over 1,000,000 new cases and 370,000 fatalities globally each year. Breast cancer diagnoses account for around 25% of all cancer diagnoses in women [1]. Choosing a suitable oncogenic target and switching to newer generations of cancer drugs is necessary due to the lack of viable and effective triple-negative breast cancer (TNBC) therapy choices [2, 3]. Even though chemotherapy is the primary treatment for TNBC, resistance is frequently encountered. In order to find novel molecular targets, a lot of study has been put into unraveling the mechanisms of TNBC drug resistance lately. Patients with TNBC, who undergo epidermal growth factor receptor (EGFR) inhibitor treatment acquire multidrug resistance (MDR). The main reason for MDR in TNBC is the non-kinetic action of EGFR1. This receptor causes the physical stabilization of sodium/glucose cotransporter 1 (SGLT1) in a mechanism outside of the receptor role, which increases glucose absorption in cancer cells. According to this mechanism, drugs that are EGFR1 receptor inhibitors lose their effectiveness to a large extent. A possible solution to overcome this problem is to eliminate the entire EGFR1 receptor protein, which is overexpressed in TNBC cells [4].

One of the advantages of gene therapy using siRNA is the capability to select and inhibit the formation of the

✉ Maliheh Safavi
m.safavi@irost.ir

[1] Department of Biotechnology, Iranian Research Organization for Science and Technology (IROST), P. O. Box 3353-5111, Tehran, Iran

[2] Department of Nanotechnology, Agricultural Biotechnology Research Institute of Iran (ABRII), Agricultural Research Education and Extension Organization (AREEO), Karaj 31535-1897, Iran

Published online: 22 May 2024

final gene product. In various diseases, this feature of siRNA with the least off-target provides researchers with a powerful tool for treating diseases [5–7]. As previously reported, mesoporous silica nanoparticles (MSNs) loaded with siRNA were used to deliver such therapies to cancer cells to resolve problems such as poor stability of siRNA in the blood, renal clearance, and limited absorption by the cells. These considerations have led to the use of siRNA in conjunction with other established gene transfer technologies [8].

During the past 20 years, magnetic nanoparticles (MNPs) have played a significant role in the delivery of drugs [9]. Their distinctive features, such as high surface-to-volume ratios and size-dependent magnetic characteristics, are very different from those of their bulk counterparts. Data storage, spintronics, catalysts, neurological stimulation, gyroscopic sensors, and other fields have all given MNPs a lot of attention recently [10–14]. One of the top concerns of the scientific community is the development of nano-therapeutics for the treatment of cancer [14]. The primary objectives of contemporary cancer therapeutic drug delivery methods are to maximize local drug concentration and minimize systemic drug distribution. To guarantee pharmacological activity with less toxicity, functionalized nanoparticle (NP) is suitable in this setting because they may inhibit the systemic metabolism and clearance of the medication [15]. Nanotechnology advancements have made it easier to deliver targeted anticancer drugs to cancer tissue in a specialized manner (receptor-mediated and ligand-mediated targeting molecules). Size and dimension affect how sensitive nanocarriers function. The physicochemical characteristics of the nanocarriers alter in response to an external stimulus, such as a change in temperature, magnetic gradient, pH, enzyme systems, or ultrasound [16, 17]. MRI contrast agents, stem cell labeling and monitoring, and target-based conveyance are just a few of the many potential applications for superparamagnetic Fe_3O_4 NPs [11, 18].

Due to our prior reports on the loading and delivery of different cargoes, including siRNA [19, 20], considering MDA-MB-231 cells as a model of TNBC, we made a magnetic nanoparticle and functionalized it with polyethylenimine (PEI), a ligand of folic acid, and polyethylene glycol (PEG). The magnetic properties of the manufactured nanoparticles make it possible to direct and accumulate the cargo in a specific position. This advantage prevents the occurrence of unwanted side effects in other tissues and organs and also greatly reduces the effective dose of the drug. We measured the FAM probe attached to the siRNAs carried by the MNP into the cell and finally calculated the amount of knockdown of the EGFR1 gene by the quantitative PCR method as a guide to the operation of the designed system. The obtained results show that such a system has been successful to a large extent in vitro and is a suitable candidate for in vivo analyses.

2 Materials and Methods

2.1 Materials

Gelest and Biopharma PEG supplied trimethoxysilylpropyl modified polyethyleneimine (PEI-silane, Mw = 1500–1800), 50% in isopropanol, and folic acid-PEG-acid (Folate-PEG-NH_2), respectively. Fluorescently tagged FAM scRNA with the sequence 50-UUC UCC GAA CGU GUC ACG UTT-30, siRNA targeting EGFR1 with four unique sequences: siR1, 50-GCG UCC GCA AGU GUA AGA ATT-30; siR2, 50-UCC ACA GGA ACU GGA UAU UTT-30; siR3, 50-CUC CAU AAA UGC UAC GAA UTT-30; siR4, 50-CCG AAA GCC AAC AAG GAA ATT-30; and a positive control against GAPDH: pcRNA, 50-UGA CCU CAA CUA CAU GGU UTT-30 were synthesized by Gene Pharma Co. Ltd. (Shanghai, China) as previously described [19]. Characterization of MNP-based nanocarriers was performed by transmission electron microscopy (TEM) at 80 kV with a Hitachi H-7650 (Japan), X-ray diffraction (XRD) with a Philips X'pert 1710 diffractometer, and Cu K (= 1.54056) in Bragg-Brentano geometry (−2). Dynamic light scattering (DLS) (Malvern Instrument, UK) technology was used to determine the size distribution of nanoparticles at 25 °C. Using a nano sizer, folded capillary cells were used to quantify the surface charge resultants (Zeta Potential) of NPs. A laminar hood was used for all cell culture techniques (Besat, Iran), and a bio-incubator was used for cell incubation (Memmert, Germany). Using an ABI 7500 thermal cycler, quantitative relative qPCR was examined.

2.2 Synthesis of PEGylated Folic Acid/β-cyclodextrin Functionalized PEI-Coated Iron Oxide Magnetic Nanoparticles (Called Fe_3O_4@βCD-PEI/FA-PEG)

With vigorous stirring, 50 mL of aqueous solution containing $FeCl_3 \cdot 6H_2O$ (10 mmol) was added to an aqueous solution (25 mL) of $FeCl_2 \cdot 4H_2O$ (5 mmol) and ammonium hydroxide (3.7 mL). Magnetic separation was carried out to separate the black precipitate, which was washed with 100 mL of water several times. Afterwards, 100 µL of NH_4OH were added, and three washes of water (50 mL each) followed by 5 min of sonication were performed. In accordance with the protocol previously reported, FA-PEG_{600}-silane was prepared [19]. FA-PEG_{600}-silane solution (0.05 g) in 10 mL isopropanol and 0.05 g PEI-silane

in 10 mL isopropanol were added consecutively to the aq. solution containing Fe_3O_4 NPs (10 mL; 4.4 mg of Fe_3O_4/mL), filtered through a sterile 0.45 µm filter after being sonicated for 10 min. A vigorous stir was then performed for 24 h. After that, the dark brown residue was separated, washed, and dried at 100 °C in a vacuum oven overnight to produce the FA-PEGylated and PEI modified magnetic nanoparticles [Fe_3O_4@PEI/FA-PEG]. To prepare [Fe_3O_4@βCD-PEI/FA-PEG], βCD was first converted to tosylated substitution using tosyl chloride (TosCl). The 5.28 mmol βCD was dissolved in 500 mL of DW, and then a solution of 15.8 mmol NaOH in 20 mL of DW was added drop by drop. The solution was then added dropwise with 30 mL of acetonitrile containing 5.28 mmol of TosCl. During 2 h at 25 °C, the reaction mixture was stirred. A white precipitate formed after the solution was acidified to pH = 3. Precipitates produced from the tosylation of βCD were filtered, desiccated for 24 h under reduced pressure, and stored at 4 °C. Following that, 1 g of tosylated βCD in 5 mL acetonitrile was added to 0.5 g Fe_3O_4@PEI/FA-PEG in 15 mL acetonitrile, and the mixture was refluxed for 24 h. Precipitate was filtered, washed with acetone, and dried under reduced pressure after reaction completion.

2.3 Gel Electrophoresis Retardation Assay

In order to assess the siRNA's capacity to bind to MNPs-based nanocarriers, gel electrophoresis was used. The buffer solutions of siRNA were combined with [Fe_3O_4@CD-PEI/FA-PEG] in varying proportions (1:0, 1:1, 1:2, 1:6, 1:12, 1:25, 1:30, and 1:50) and incubated for 24 h at 4 °C. Following the mixing of staining buffer with Tris/acetate/EDTA (TAE) running buffer (1 L), the mixtures were run on a 2.5% agarose gel at 100 V for 45 min. Utilizing Bio-Rad imaging equipment and a gel documentation system [21], RNA bands were photographed and observed under UV light.

2.4 Optimization of the siRNA Loading

To improve the siRNA loading in [Fe_3O_4@βCD-PEI/FA-PEG], the impacts of two factors, such as temperature and loading duration, were examined with a ratio of 1:30 of siRNA/Fe_3O_4@CD-PEI/FA-PEG. In a 2 mL centrifuge tube, siRNA and [Fe_3O_4@βCD-PEI/FA-PEG] were dispersed in water. The mixture was vortexed for 40 s before being shaken at 280 rpm continuously for 1 and 24 h at 4 °C, as well as 1 and 24 h at 25 °C. The siRNA@[Fe_3O_4@βCD-PEI/FA-PEG] was separated from the solid residual by centrifuging it at a speed of 20,000 g for 15 min or using a magnet. The amount of siRNA molecules in the supernatant was measured using an Epoch Microplate Spectrophotometer (BioTek) using Microvolume Take3 plates.

2.5 siRNA Release Assay

According to the Liu et al. protocol [22], siRNA release from MNP was evaluated in TE buffer. In RNase-free Eppendorf 2.0 mL containers, siRNA@[Fe_3O_4@CD-PEI/FA-PEG] was incorporated into 200 µL TE buffer and maintained at 37 °C with horizontal 120 rpm/min stirring. At predetermined intervals, the tubes were centrifuged at 12,000 rpm (4 °C for 30 min). After re-dispersion into fresh TE buffer, siRNA@[Fe_3O_4@CD-PEI/FA-PEG] pellets were re-incubated for intermittent or non-continuous determination. An Epoch Microplate Spectrophotometer (BioTek) was used to measure the amount of siRNA molecules in the supernatant.

2.6 Gel Electrophoresis and RNase Protection Assays

The siRNA@[Fe_3O_4@βCD-PEI/FA-PEG] was introduced to the RNase in solution after being washed with PBS to explore the protective impact of the siRNA by [Fe_3O_4@βCD-PEI/FA-PEG] against RNase. After incubating for 1 h with 0.25% RNase A (Takara), the mixture was run at 90 V for 40 min. Prior to gel electrophoresis, mixtures were treated with 0.6 U/mg of heparin per mg of siRNA in DEPC-treated water to disentangle the siRNA from the noncomplex.

2.7 Cell Culture

The MCF-10 A and MDA-MB-231 cell lines of human normal and cancerous breast tissue, respectively, were bought from the National Cell Bank of Iran (NCBI) and grown in RPMI 1640 (Gibco) at 37 °C and 5% CO_2. RPMI 1640 medium was supplemented with 10% heat-inactivated fetal bovine serum (FBS, Biosera), 100 mg/mL streptomycin, and 100 U/mL penicillin.

2.8 Cell Survival Assay

By using the MTT [3-(4, 5-dimethylthiazol-2-yl)-2, 5-diphenyl tetrazolium bromide] test in triplicate, the anti-proliferation activity of [Fe_3O_4@βCD-PEI/FA-PEG] was assessed. In a 96 well microplate, 190 µL of RPMI 1640 were used to seed roughly 1×10^4 cells per well overnight. Serially diluted [Fe_3O_4@βCD-PEI/FA-PEG] that was prepared in culture media free of serum was applied to the cells for transfection. Negative controls were thought to be non-transfected cells. Two hundred microliter of phenol red-free media containing MTT (1 mg/mL) was added to each well following the removal of the medium. An additional 4 h of incubation at

5% CO_2, 90% humidity, and 37 °C were then conducted on the plates. The formazan crystals were dissolved in 100 µL of DMSO, and then the absorbance at 570 nm was measured by a microplate reader (Epoch, BioTek). The tests were run three times.

2.9 Cellular Uptake Studies

Overnight, 3×10^5 MDA-MB-231 cells were seeded in a 6-well plate to evaluate siRNA uptake by the cells. Fresh low serum RPMI 1640 was used as the culture medium, and it was loaded with a [Fe_3O_4@βCD-PEI/FA-PEG] combination of FAM-labeled siRNA. Infusion of the cells for 4 h was followed by trypsinization, collection, and resuspension in PBS. An intracellular absorption measurement of siRNA-MNP labeled with FAM (FL1, 525 nm) was performed in less than 1 h using a flow cytometer (Sysmex Cyflow Space, Japan).

In order to observe siRNA in the cytosol, confocal laser scanning microscope (CLSM) was used. The MDA-MB-231 cells were seeded 1 day before transfection in RPMI-1640 culture media on a coverslip in a 35-mm culture plate. At the time of transfection, the cells were exposed to siRNA@[Fe_3O_4@βCD-PEI/FA-PEG] for 4 h, and after washing twice with PBS were fixed and stained with LysoTracker Deep Red according to the previously described method [19]. Finally, imaging was performed by CLSM (Zeiss, Germany).

2.10 In VitroEGFR1 Silencing

The purification of RNA was carried out according to a previously reported method [23]. To purify total RNA, the QIAGEN RNeasy Kit was used to collect cells, and the manufacturer's instructions were followed for the remaining processes. Using a NanoDrop Spectrophotometer, the concentration of pure mRNA was determined (Biotek, Japan). One hundred nanograms of mRNA was reverse-transcribed to complementary DNA (cDNA) using a reverse transcription and cDNA synthesis kit from QIAGEN. First-strand cDNA (M-MuLV) was created using reverse transcriptase. An intercalated SYBR green dye-based qPCR was performed using a 20 µL reaction in accordance with the manufacturer's instructions (Ampliqon, Denmark). In summary, each well received 10 µL of the master mix, 4 µL of primers (10 pMol), 2 µL of template cDNA (1.5 g/L), and 4 µL of ddH_2O. The qPCR result was obtained by the fluorescent intensity emitted due to amplification of a piece (78 nt) of the homo sapiens EGFR1 (NM_005228.5) mRNA and GAPDH (NM_001256799) mRNA using exon junction forward and reverse specific primers, FEGFR: 5′-AGG TGG TCC TTG GGA ATT TG -3′, REGFR: 5′-CCT CCT GGA TGG TCT TTA AGA AG -3′, FGAPDH: 5′- CTG GGC TAC ACT GAG CAC C -3′, and RGAPDH: 5′- AAG TGG TCG TTG AGG GCA ATG-3′. Raw data obtained from amplification was normalized to GAPDH as the reference gene and represented as Cq values. The rapid PCR was then run for 40 cycles using the following protocol: activation for 3 min at 95 °C, denaturation for 15 s at 95 °C, and annealing and extension for 1 min at 60 °C. The exon junction forward and reverse specific primers, FEGFR (as reported in our previous work [19]), were used to perform the quantitative raw data from amplification and were displayed as Cq values after being adjusted to GAPDH as the reference gene.

An ABI 7500 real-time PCR equipment was used to run each qPCR reaction in triplicate. The comparative 2-CT (2-Cq) approach was used to examine the expression of EGFR1 and the precise level of gene knockdown. After 24 and 48 h of siRNA incubation, a knockdown percentage was determined using Cq with a 0.05 threshold. Using previously published data, the gene knockdown level was determined. The ratio of the target gene to the reference gene was used to depict the results. *C*q is equal to *C*q (treated) − *C*q (control), where *C*q for treated cells is equal to *C*q treated (EGFR1 in treated cells) − Cq (GAPDH in treated cells) and *C*q control (EGFR1 in untreated cells) − *C*q (GAPDH in untreated cells). As a result, the extent of knockdown is determined as a percentage of the level of gene expression.

2.11 Statistics

Data were analyzed using GraphPad Prism version 8.4.2 (GraphPad Software, Inc., San Diego, CA). Statistical significance was assessed by one-way ANOVA and Kruskal-Wallis (for qPCR results). $P < 0.05$ was considered the significance criterion. The date was represented as a bar graph (mean and standard deviation).

3 Results and Discussion

3.1 Preparation and Characterization of Nanocarrier

A nanocarrier based on MNP was created in the current study. By adding additional positive charge to the nanoparticle through PEI functionalization for utilization, such as efficient transfection and endosomal escape, we were able to accomplish the study's objective. MNPs are the perfect nano-platform for creating intelligent drug delivery systems for biological applications [24].

MNPs have a high capacity for drug loading, exhibit stimulus-responsive drug release behaviors, and also show high biocompatibility. MNPs are also relatively simple to multi-functionalize [25].

To attach negatively charged siRNA to MNP and increase cellular uptake, positively charged organic chemicals, such as PEI or poly-l-lysine (PLL) [26–28], are typically used to treat nanocarriers. So, cationic polymers like PEI were added to the [Fe_3O_4@βCD-PEI/FA-PEG]] in this study to make it positively charged so that it could bind to siRNA electrostatically.

Furthermore, PEI promotes endosomal escape of nanoparticles through the "proton sponge effect" which depends on an increase in H^+ concentrations during endosomal hydrolysis [27, 29, 30]. Cationic PEI causes a rise in membrane potential and counter-ions to enter, which causes the endosome to enlarge and rupture and ultimately release siRNA into the cytoplasm before being introduced to the lysosomes [31, 32].

Regarding the specific properties of MNPs, these NPs are a promising nanomaterial family for developing a nano-delivery system for the efficient transferring of different biological cargoes. The biocompatibility and potential of the MNPs-based nanocarrier for siRNA delivery were investigated. To this, Fe_3O_4 NPs were synthesized, and its surface was functionalized by grafting the multi-functional groups including PEI functionalized β-cyclodextrin (βCD-PEI) and PEGylated folic acid (PEG-FA) in order to obtain the Fe_3O_4@βCD-PEI/FA-PEG nanocarrier. The biodegradable PEG and βCD functionalized PEI moieties were chosen to improve the biocompatibility and loading/releasing efficiency of the nanocarrier. The nanostructures were characterized using XRD, TGA, TEM, SEM, atomic force microscopy (AFM), and zeta potential analysis. Schematically, the [Fe_3O_4@βCD-PEI/FA-PEG] NPs were prepared as shown in Fig. 1.

The shape and particle size of the [Fe_3O_4@βCD-PEI/FA-PEG] nanocarrier were determined with SEM and TEM (Fig. 2a, b). The MNPs-based nanocarrier showed spherical particles with an average size below 60 nm. Previous studies have shown that NPs should be smaller than 75 nm in size in order to transport genes effectively [33, 34]. Therefore, the [Fe_3O_4@βCD-PEI/FA-PEG] nanocarrier is a perfect fit for transporting biomolecules. An identical 3D topography for the [Fe_3O_4@βCD-PEI/FA-PEG] and siRNA@[Fe_3O_4@βCD-PEI/FA-PEG] samples has been confirmed by the AFM images (Fig. 2c). The superparamagnetic features of the nanocarrier were determined using a vibrating sample magnetometer (VSM) before and after modification, and the saturation magnetization curves of MNPs and [Fe_3O_4@βCD-PEI/FA-PEG] are presented in Fig. 2d. The saturation magnetization value of pure Fe_3O_4 MNPs was ~ 50 emu g^{-1} which decreased to ~ 35.4 emu g^{-1} after the modification process with the βCD-PEI and FA-PEG polymers.

For [Fe_3O_4@βCD-PEI/FA-PEG] and siRNA@[Fe_3O_4@βCD-PEI/FA-PEG] samples, XRD examination verified that the MNPs with the peaks featuring [220], [311], [400], [422], [511], and [440] reflections were detected at 2Θ = 30°, 35.2°, 44.7°, 54.6, 57.01, and 62.5°, respectively. This outcome demonstrated that the magnetic characteristic was retained upon the siRNA loading process (Fig. 2e). The zeta potential measurement for nanomaterials at pH 7 showed that the surface charge of the Fe_3O_4, [Fe_3O_4@βCD-PEI/FA-PEG], and siRNA@[Fe_3O_4@βCD-PEI/FA-PEG] samples were about −10.5, 29, and 18.1 mV, respectively. The siRNA@[Fe_3O_4@CD-PEI/FA-PEG] complex was formed because of the electrostatic interaction between the positive PEI and βCD and the negative siRNA. The zeta potential in [Fe_3O_4@βCD-PEI/FA-PEG] was reduced by this interaction from 29 to 18.1 mV in the siRNA@[Fe_3O_4@βCD-PEI/FA-PEG]. The siRNA was able to securely interact with its surface because of the positively charged [Fe_3O_4@βCD-PEI/FA-PEG] caused by PEI and βCD groups. As a consequence, siRNA is effectively delivered to cancer cells while being preserved by PEI and βCD (Fig. 2f). TGA diagrams of the uncoated MNPs, [Fe_3O_4@PEI/FA-PEG], and siRNA@[Fe_3O_4@βCD-PEI/FA-PEG] confirmed the successful grafting of β-CD-PEI and FA-PEG on the magnetic surfaces. The average grafting contents of Fe_3O_4 (including SiO_2 layer come from polymeric precursors), βCD, and PEI-FA-PEG polymers on the [Fe_3O_4@βCD-PEI/FA-PEG] were ~ 25%, 45%, and 25%, respectively, measured from the weight loss of the samples (Fig. 2g).

3.2 Gel Retardation Assay

One of the prerequisites for carriers in gene therapy is MNPs' capacity to attach to nucleic acids. Using the gel electrophoresis retardation test allowed researchers to look into how the complex's constituent parts connected to siRNA and came together to create the final complex. In this technique, a 2.5% agarose gel was used to load the siRNA@[Fe_3O_4@CD-PEI/FA-PEG] final complex at different ratios of MNP to 1.38 μg of siRNA. Complexes with positive or neutral net charges are unable to move closer to the positive pole as polymer-to-siRNA ratios increase. As a result, siRNA was overwhelmed by the polymer's positive charge, so in the well, the complex remained immobile. Although in smaller amounts, it was unable to completely stop the nucleic acid's mobility on the gel from being delayed. This finding suggests that siRNA binds the βCD and PEI groups with suitable affinity. According to the theory, complexes will not move if the net charge of (siRNA@[Fe_3O_4@βCD-PEI/FA-PEG]) becomes neutral (or positive) when the [Fe_3O_4@βCD-PEI/FA-PEG] ratio increases. Simultaneously, siRNA may transfer to the gel's positive electrode if the MNP ratio is insufficient to provide enough positive charge to offset siRNA's negative charge. It has been demonstrated categorically that [Fe_3O4@CD-PEI/FA-PEG] is completed when siRNA is added at a ratio of 1:30 (or higher ratios) to the complex (Fig. 3a).

3.3 siRNA Loading Efficiency in [Fe3O4@βCD-PEI/FA-PEG]

Optimizing siRNA loading in the [Fe_3O_4@CD-PEI/FA-PEG] nanocarrier was investigated by analyzing the effects of a 1:30 ratio of siRNA/MNPs during two distinct time periods (1 and 24 h) at 4 and 25 °C. UV absorption measurements were used to assess the ratios, reaction temperature, and incubation time to improve the siRNA's capacity to load for usage in cell research. The concentration of unbounded siRNA was determined when [Fe_3O_4@βCD-PEI/FA-PEG] was incubated with siRNA. Different options were studied by taking temperature and time factors into account in order to find the best way to prepare the siRNA@[Fe_3O_4@βCD-PEI/FA-PEG]. The optimal incubation time for nucleic acid with nanoparticles was 24 h at 4 °C. It was determined that 86% of the initial nucleic acid amount had interacted with the nanoparticles through the use of a nanodrop to measure the supernatant after centrifuging the mixture (Fig. 3b).

3.4 Release of siRNA from siRNA@[Fe_3O_4@βCD-PEI/FA-PEG]

At various time points in the TE buffer, the siRNA release behavior of [Fe_3O_4@βCD-PEI/FA-PEG] was examined. Most likely, siRNA diffusion via the MNPs matrix and the gradual erosion of MNPs matrix or disintegration were the main contributors to the released phase in the release assay [35, 36]. This molecule is suggested as a potential drug carrier because of the delayed release that was seen, which would be perfect for our goal.

By measuring the proportion of siRNA released from [Fe_3O_4@CD-PEI/FA-PEG] in relation to the initial quantity of siRNA loaded into the MNPs, siRNA release profiles were obtained in vitro. siRNA had a lag-time continual release after its initial release (Fig. 3c). After 120 h, siRNA-MNP had cumulatively released siRNA at a rate of around 78%. These results show that manufactured nanocarriers have slow-release characteristics. Various time periods were used to determine the quantity of siRNA released in the supernatant. In the non-continuous process of this study, the supernatant was fully discarded after detecting the nucleic acid concentration and was replaced with the same volume of TE buffer.

3.5 Evaluation of siRNA Protection from RNase A

The ability of [Fe_3O_4@βCD-PEI/FA-PEG] to shield siRNA from RNase enzymatic cleavage was confirmed using agarose gel electrophoresis analysis. siRNA@[Fe_3O_4@CD-PEI/FA-PEG] (siRNA 1:30 MNP) was exposed to RNase A (Fig. 4, Lanes 4 and 5) or RNase A followed by heparin (Lanes 6 and 7) in order to determine the protective effect of siRNA via MNP. The movement of bare siRNA over the gel is shown in Lane 2. As a result of the RNase A treatment in Lane 8, bare siRNA was degraded. After two steps of 6 h incubation, the siRNAs coupled to [Fe_3O_4@βCD-PEI/FA-PEG] exhibited no signs of degradation and were maintained in the wells (Lanes 4 and 5). After 2 and 6 h of RNase incubation, siRNA@[Fe_3O_4@βCD-PEI/FA-PEG] were treated with heparin, and abundant siRNA release was seen in Lanes 6 and 7.

After 6 h of RNase incubation, our tests revealed that [Fe_3O_4@βCD-PEI/FA-PEG] exhibited a considerable level of protective effectiveness. Although no specific siRNA orientation is necessary, the fact that PEI also coats the outside surface of nanopores makes certain bound siRNA more likely to attach to it. Additionally, the substantial positive charge of PEI can protect it from nuclease activities.

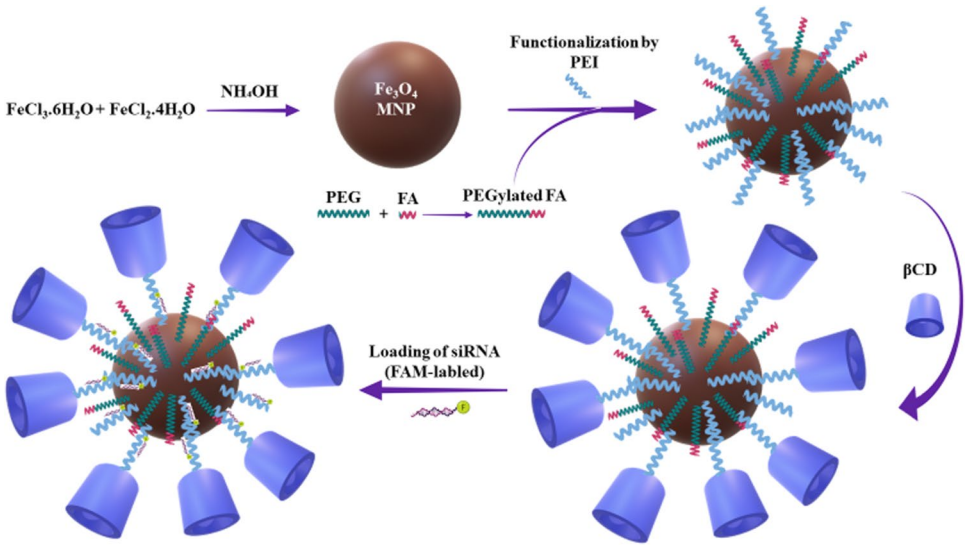

Fig. 1 Schematic figure of the synthesis and functionalizing of the magnetic nanoparticle

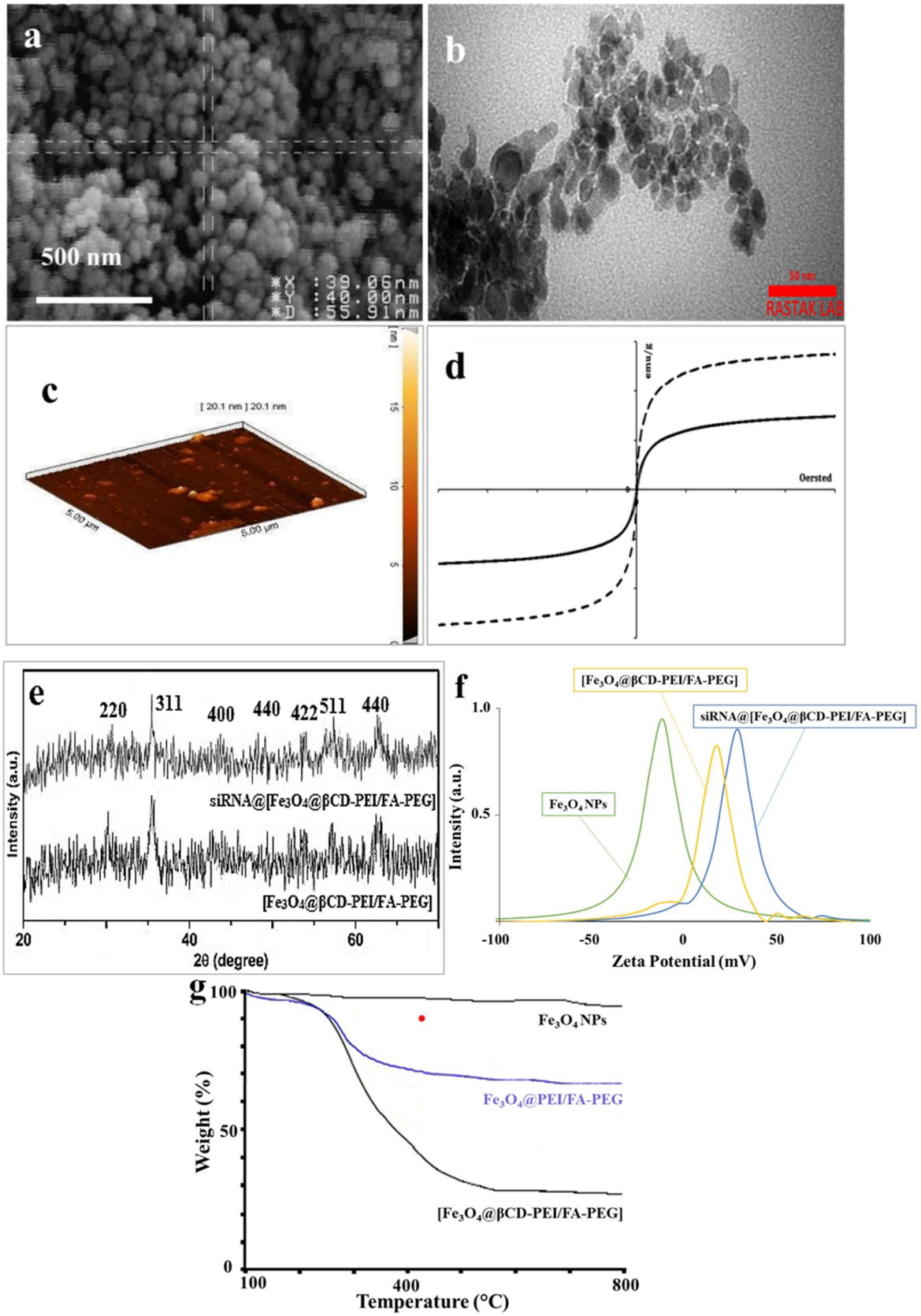

Fig. 2 Characterization of MNP vehicles: SEM (**a**), TEM (**b**), AFM (**c**), VSM (**d**), XRD (**e**), zeta potential measurement (**f**), and TGA (**g**) results of siRNA@[Fe_3O_4@βCD-PEI/FA-PEG]

3.6 Cytotoxicity of [Fe_3O_4@βCD-PEI/FA-PEG]

The [Fe_3O_4@βCD-PEI/FA-PEG] was predicted to have minimal cytotoxicity, so it might be employed as a siRNA delivery nanocarrier as a biocompatible vehicle. The effects of this compound, [Fe_3O_4@βCD-PEI/FA-PEG], on cell proliferation were investigated by MTT test. Figure 5a, b displays the outcomes of 24 and 48 h of MNP incubation on the breast cancer cell line, MDA-MB-231, and breast normal cell line, MCF-10 A. The [Fe_3O_4@βCD-PEI/FA-PEG] exhibits exceptional cytocompatibility by indicating no detectable cytotoxicity against both cancer and normal cell lines at tested dosages.

3.7 Flow Cytometer Analysis of siRNA@[Fe_3O_4@βCD-PEI/FA-PEG]

MNP, as a nanocarrier, must be absorbed by the cell in order to properly transport loaded siRNA into cancer cells. The MDA-MB-231 cancer cells were collected after 6 h of incubation with FAM-labeled siRNA loaded in [Fe_3O_4@βCD-PEI/FA-PEG]. The findings show that after 6 h of incubation of cells, the rate absorption of (siRNA@[Fe_3O_4@βCD-PEI/FA-PEG]) reached 62.6% when using a magnet in comparison with the cells incubated without using the magnet, with cellular uptake of 44.6% (Fig. 5c).

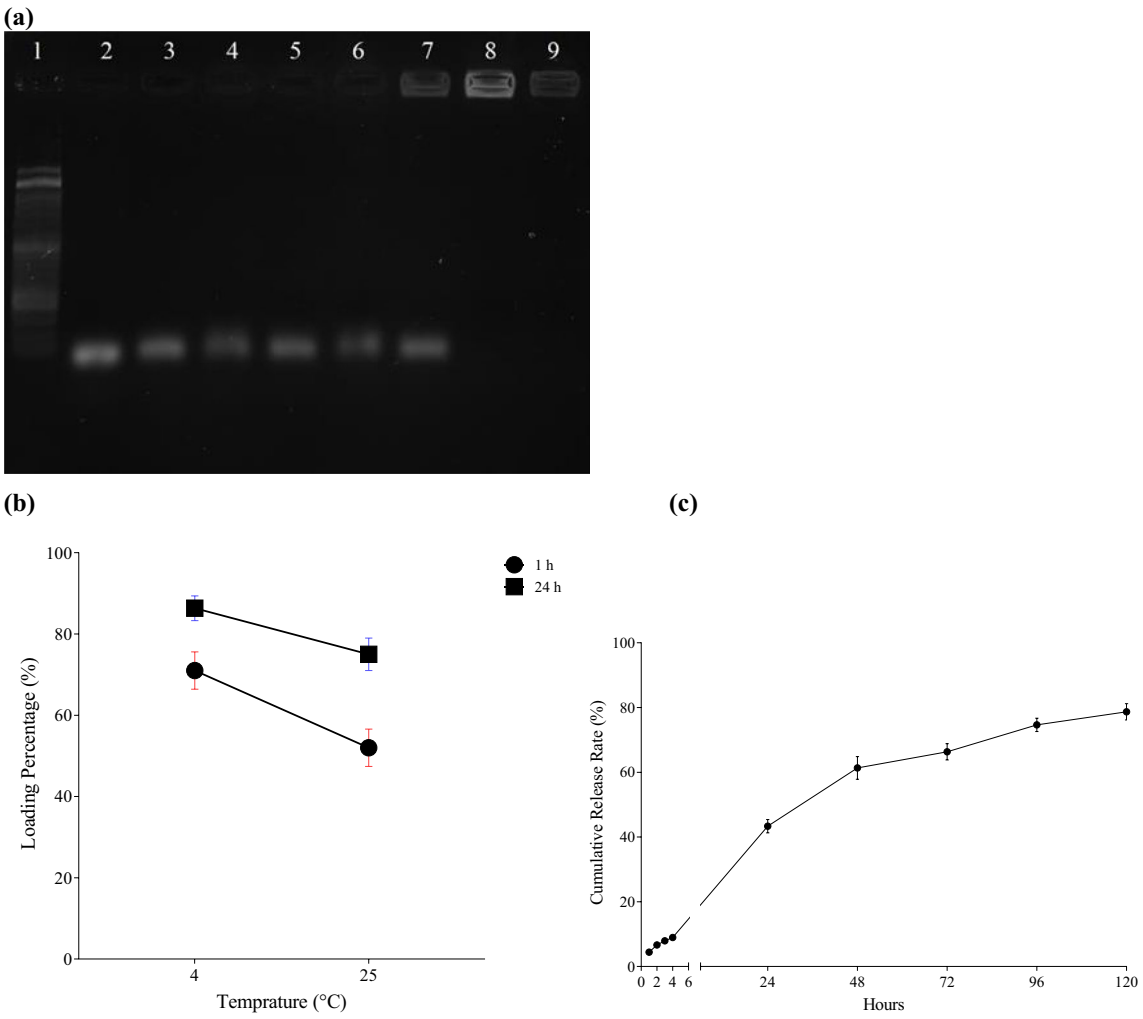

Fig. 3 **a** Retardation assay of siRNA@[Fe_3O_4@CD-PEI/FA-PEG] at different concentrations using gel electrophoresis. Marker 50 bp (Lane 1), naked siRNA (Lane 2), ratio 1:1 (Lane 3), ratio 1:2 (Lane 4), ratio 1:6 (Lane 5), ratio1:12 (Lane 6), ratio 1:25 (Lane 7), ratio 1:30 (Lane 8), and ratio 1:50 (Lane 9). All proportions are according to (siRNA: [Fe_3O_4@βCD-PEI/FA-PEG]). **b** siRNA loading profile on [Fe_3O_4@CD-PEI/FA-PEG] nanocarrier incubated for 1 and 24 h at 4 and 25 °C. The best loading results of the final complex were achieved to 86% of loading in 24 h of incubation at 4 °C using a ratio of 1:30 of siRNA to [Fe_3O_4@CD-PEI/FA-PEG], equating to 2.1 μM siRNA in combination with 41.4 μg of [Fe_3O_4@CD-PEI/FA-PEG]. **c** The siRNA release from the [Fe_3O_4@βCD-PEI/FA-PEG] at 37 °C. Data are given as the means ± S.D. ($n = 3$)

The difference of 18% in delivering siRNA to the cytosol indicates the effectiveness of the magnetic property of the nanoparticle as a tool for carrying nucleic acid in gene therapy. As compared to other nonviral nucleic acid delivery systems, like Lipofectamine 2000 and PEI/siRNA complexes [37], PEI-MNP showed almost the same results but significantly less cytotoxicity in cells, demonstrating that PEI-MNPs provide a desirable method for siRNA delivery.

The dosage of transfection is preferable based on MDA-MB-231 cell line research [38, 39], which contrasts with other studies. Note that different cell lines respond differently to transfection reagents. For MDA-MB231 cells, which are among the most challenging to transfect, this rate is predicted to reach up to 55% when using commercial transfection reagents. The presence of a positive surface charge generated by PEI may perhaps account for the increased cellular uptake seen in the MNP-based nanocarrier developed in this study. By creating a connection between the negatively charged cell surface and the positively charged nanoparticles, endocytosis is encouraged. According to the proton sponge hypothesis, this positive charge promotes endosomal escape inside the cell.

3.8 Localization and Endosomal Escape

Utilizing folate ligand also enhances the high nanocarrier distribution to breast cancer cells. On the surface of cancer cells, the folate receptor is overexpressed, which might be used as a marker in studies. The use of this molecule is appealing to researchers since it is inexpensive and stable over a wide range of temperatures. Yet, its best feature is to increase cellular uptake, which enhances transfection yield and causes receptor-mediated endocytosis in addition to the passive transfer of nanoparticles [40–42].

The efficiency of transfection and delivery of the cargo to the cytosol in gene therapy is one of the basic criteria of a nanocarrier. Therefore, it is necessary to escape the drug being transported from the lysosome and prevent lysosomal digestion to make a suitable nanocarrier. In order to assess this, MDA-MB-231 cells transfected with nanoparticles containing labeled siRNA (siRNA@[Fe_3O_4@βCD-PEI/FA-PEG]) with FAM were fixed and stained with LysoTracker Red after 4 h of exposure to the cells. Finally, the CLSM images recorded the presence of siRNA in the cytosol with a green color next to the red color of lysosomes (Fig. 5d).

The presence of siRNA in the cytosol was confirmed by differential staining of lysosomes and nuclei in confocal microscopy. Fluorescent label attached to siRNA (FAM) with optimal distance from lysosomes indicates lysosomal escape after 6 h that occurred due to nanoparticle charge based on proton sponge hypothesis due to PEI and βCD.

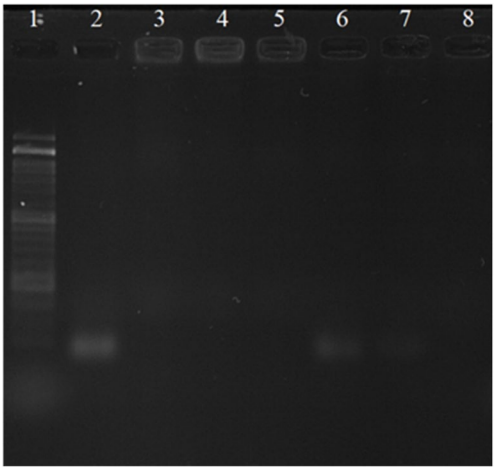

Fig. 4 RNase protection assay for the protective effect of [Fe_3O_4@βCD-PEI/FA-PEG] on siRNA. Lane 1: DNA Ladder (50 bp); Lane 2: naked siRNA; Lane 3: siRNA@[Fe_3O_4@βCD-PEI/FA-PEG] (1:30); Lane 4: siRNA@[Fe_3O_4@βCD-PEI/FA-PEG] + RNase, 2 h; Lane 5: siRNA@[Fe_3O_4@βCD-PEI/FA-PEG] + RNase, 6 h; Lane 6: siRNA@[Fe_3O4@βCD-PEI/FA-PEG] + RNase, 2 h + then heparin: Lane 7: siRNA@[Fe_3O_4@βCD-PEI/FA-PEG] + RNase, 6 h + then heparin; Lane 8: naked siRNA incubated with RNase

3.9 EGFR1 Gene Knockdown

The qPCR test as an indicator of the performance of the [Fe_3O_4@βCD-PEI/FA-PEG] complex shows a significant difference in the knockdown of the EGFR1 gene with and without the use of a magnet during transfection. Using RT-qPCR, the EGFR1 gene expression level was investigated. The transcription levels of EGFR1 in the tested cells were assessed 48 h after transfection in two groups (with and without magnet administration) and compared with their untreated counterparts. A measure of the EGFR1 expression levels was conducted and normalized to the levels of endogenous transcripts in untreated cells. Based on the data, EGFR1 mRNA was significantly knocked down by a cocktail of siRNAs (mix), 66% without and 78% with administration of magnet after 48 h of transfection of cells (Fig. 6). All other groups (siR1, siR2, siR3, siR4) show no significant knockdown in EGFR1 mRNA.

The observed reduction in EGFR1 mRNA levels serves as evidence that all experimental steps, encompassing siRNA functionality, endosomal escape, and cellular uptake, were executed accurately. Therefore, it may be concluded that the in vitro gene delivery procedure is acceptable and that the gene therapy system can proceed with in vivo procedures. The cytotoxicity of the PEI/siRNA complexes has hindered in vivo applications, despite their usage for non-viral gene delivery. But the siRNA@[Fe_3O_4@CD-PEI/FA-PEG] complex has a high affinity for encapsulation, demonstrates biocompatibility, and, as previously mentioned, facilitates the efficient transport of the payload.

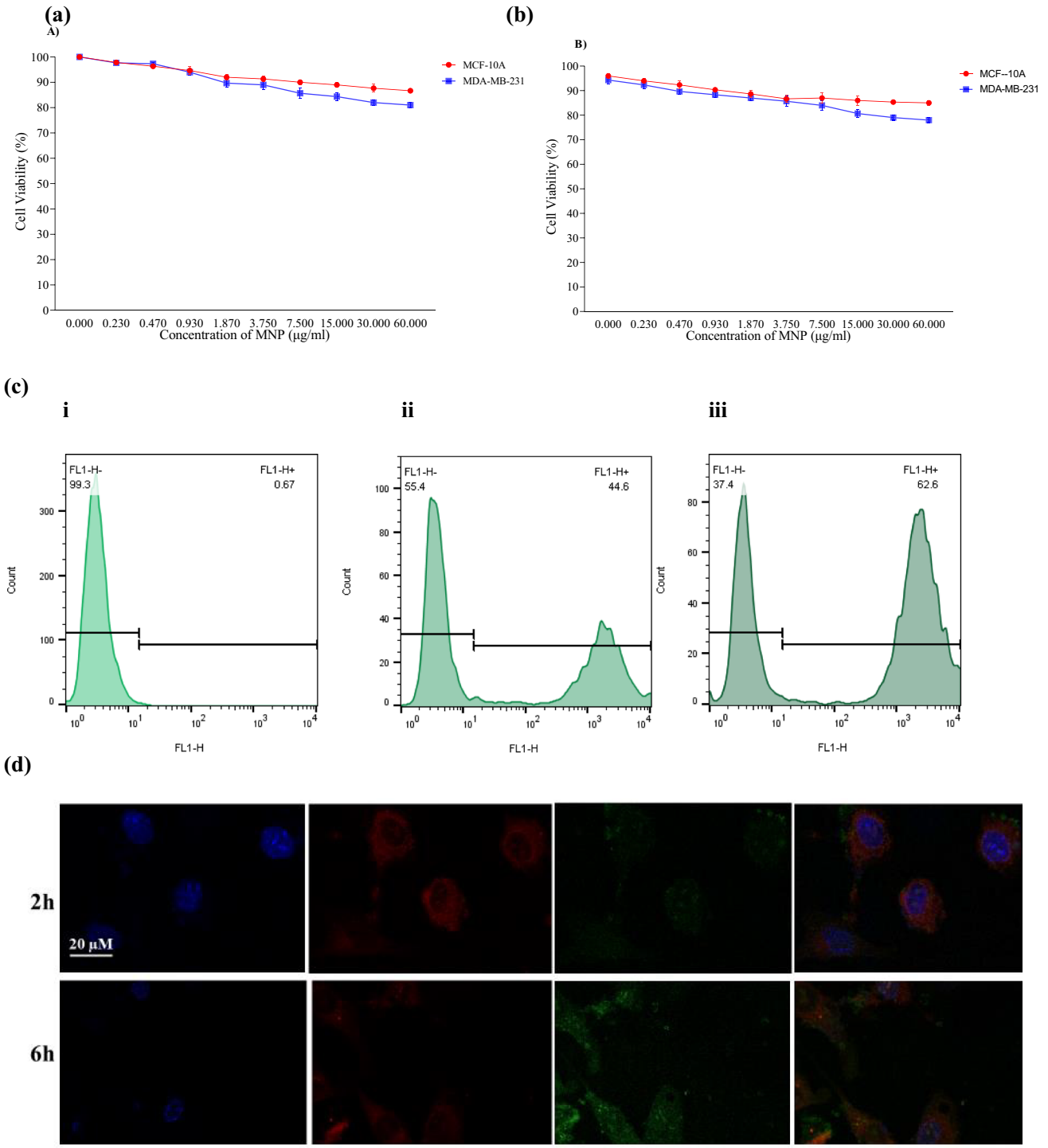

Fig. 5 *In vitro* biocompatibility of [Fe_3O_4@βCD-PEI/FA-PEG], uptake, localization, and endosomal escape of siRNA@[Fe_3O_4@βCD-PEI/FA-PEG]). The viability of MDA-MB-231 and MCF-10 A cells after 24 h (**a**) and 48 h (**b**) of treatment with various doses of [Fe_3O_4@βCD-PEI/FA-PEG]. (**c**) MDA-MB-231 cells incubated with siRNA@[Fe_3O_4@βCD-PEI/FA-PEG] were analyzed using flow cytometry: (i) negative control cells treated with PBS, (ii) cells treated with FAM-labeled siRNA@[Fe_3O_4@βCD-PEI/FA-PEG] for 6 h without magnet, (iii) cells treated with FAM-labeled siRNA@[Fe_3O_4@βCD-PEI/FA-PEG] for 6 h with magnet. (**d**) Confocal images of MDA-MB-231 cells that were exposed to siRNA@[Fe_3O_4@CD-PEI/FA-PEG] for 2 and 6 h with magnet. FAM (green), DAPI (blue), and LysoTracker (red) were used to label the NPs, nucleus, and endosomes, respectively

4 Conclusions

For developing siRNA nanocarriers, a variety of criteria are taken into consideration, including those pertaining to the intended use of the conveyance in addition to those pertaining to the payload. Using the most essential factors of siRNA loading into nanocarriers, the current study designed distinct magnetic nanocarriers that are optimized for cell uptake, have the optimal amount of siRNA for cellular uptake, and do not have dose-related off-target effects. A siRNA@[Fe_3O_4@βCD-PEI/FA-PEG] complex was created in order to effectively knock down the EGFR1 gene, which is the final step in the self-efficacy pathway.

In treatment, especially targeted gene therapy, one of the biggest problems is the lysosomal degradation of drugs once they get into the cytosol. The use of a vehicle with a tampon capacity and pregnancy led to the escape of the dose, which increases the effectiveness and efficiency of the cargo (siRNA) and also reduces the effective dose. Endosomal escape has happened due to the compound's buffering capability and excellent functionalization of nanoparticles. By designing and using magnetic fields in the area of the target organ or tissue, both with local and general administrations, the drug can be directed to the target site and concentrated there. Such targeted drug delivery greatly reduces the dose used and also prevents the unwanted effects of the drug on flanked tissues.

Last but not least, all modifications, including functionalization with PEI and βCD, have the potential to be extremely impactful, particularly in the case of EGFR1 gene knockdown and in vitro cellular uptake. Research in this sector intends to develop an optimum and durable functionalized nanoparticle for gene therapy for different diseases by utilizing a variety of siRNA sequences.

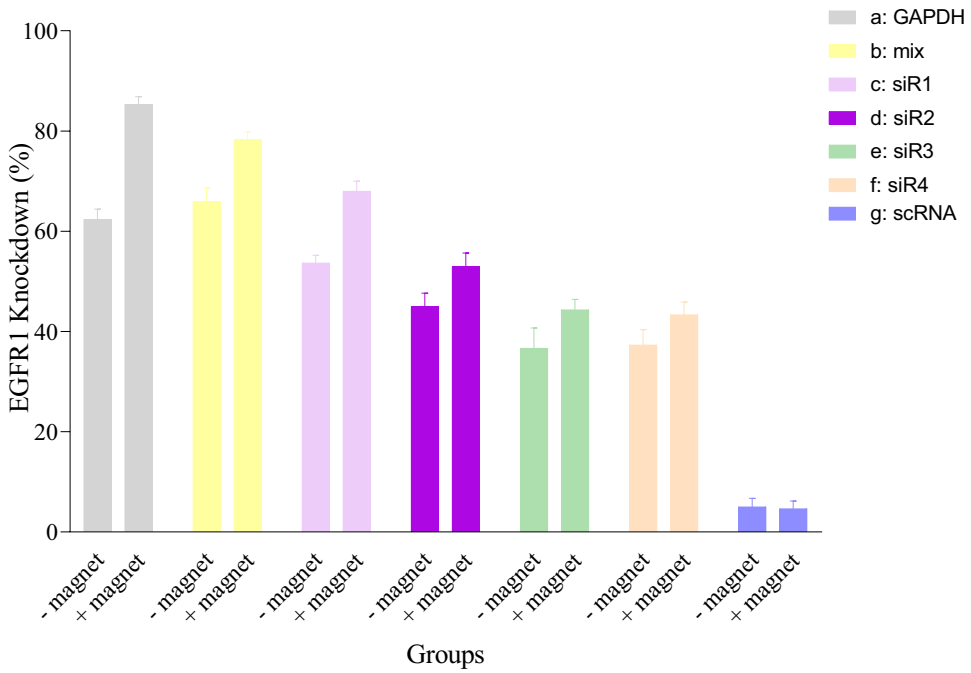

Groups	Without magnet		With magnet	
	Mean ± SD	P- value	Mean ± SD	P- value
GAPDH	62.33 ± 2.08	**0.013**	85.33 ± 1.52	**0.002**
mix	66.00 ± 2.64	**0.003**	78.33 ± 1.52	**0.018**
siR1	53.67 ± 1.52	0.10	68.00 ± 2.00	0.10
siR2	45.00 ± 2.64	0.45	53.00 ± 2.64	0.45
siR3	36.67 ± 4.04	>0.99	44.33 ± 2.08	>0.99
siR4	37.33 ± 3.05	>0.99	43.33 ± 2.51	>0.99
scRNA	5.00 ± 1.73		4.66 ± 1.52	

Fig. 6 Real-time quantitative PCR of MDA-MB-231 cells 48 h after transfection of siRNA@[Fe 3 O 4 @βCD-PEI/FA-PEG] with and without administration of magnet. **a** As a positive control (GAPDH), RT-qPCR analysis shows about 85% knockdown, **b** as a cocktail of siRNAs (mix) about 78% knockdown, **c** as siR1 about 68% knockdown, **d** as siR2 about 53%, **e** as siR3 about 44%, and **f** as siR4 about 43% knockdown; **g** in the case of scrambled RNA (scRNA), no significant change in expression level was observed (siR1, siR2, siR3, and siR4 are different siRNA molecules that target EGFR1, and scRNA is scrambled RNA)

Fe_3O_4 nanoparticles without targeting ligand enter the cells by endocytosis mechanism. In this study, FA ligand, which targets the folic acid receptor, was used to increase cell absorption and also to increase the accuracy of targeting cancer cells. This receptor is expressed more on the surface of cancer cells than normal cells.

Considering the importance of in vivo studies, further studies in this field will solve many problems. In this case, it is desirable to predict the bio-distribution of magnetic nanoparticles. According to the reported studies, after the intravenous injection of Fe_3O_4 nanoparticles into mice, using X-ray scanning analytical microscopy (XSAM) and magnetic resonance imaging (MRI), the nanoparticles were immediately distributed in the bloodstream and observed in the liver, spleen and kidney [43].

Author Contribution Author contribution: JP: methodology, formal analysis, writing—original draft. LM: conceptualization, project administration, validation, and review and editing. MRB: visualization. MS: supervision, conceptualization, project administration, validation, and review and editing.

Funding This work was supported by the Cancer Control Research Center, Cancer Control Foundation, Iran University of Medical Sciences, Tehran, Iran (grant no. CCF-98035).

Data Availability The datasets that support the findings of the current study are available on reasonable request from the corresponding author.

Statistics: GraphPad Prism version 8.4.2. was used to analyze the data. An analysis of variance (ANOVA) and Student's *t*-test were used to assess statistical significance. A significance cutoff of P 0.05 was used. A bar graph showed the date (mean and standard deviation).

Declarations

Ethics Approval and Consent to Participate Not applicable.

Informed Consent Not applicable.

Conflict of Interest The authors have no conflict of interests.

Research Involving Humans and Animals Statement Not applicable. This article does not contain any studies with human participants or animals performed by any of the authors.

References

1. Azari, M., Bahreini, F., Uversky, V. N., & Rezaei, N. (2023). Current therapeutic approaches and promising perspectives of using bioengineered peptides in fighting chemoresistance in triple-negative breast cancer. *Biochemical Pharmacology*, *210*, 115459.
2. O'Reilly, E. A., Gubbins, L., Sharma, S., Tully, R., Guang, M. H. Z., Weiner-Gorzel, K. The fate of chemoresistance in triple negative breast cancer (TNBC) [Internet]. BBA Clin. 2015 [cited 2021 May 1]. pp. 257–75. https://www.sciencedirect.com/science/article/pii/S2214647415000173.
3. Penault-Llorca, F., & Viale, G. (2012). Pathological and molecular diagnosis of triple-negative breast cancer: A clinical perspective. Annals of Oncology [Internet]. [cited 2021 May 1];23. https://www.sciencedirect.com/science/article/pii/S0923753419376380.
4. Weihua, Z., Tsan, R., Huang, W. C., Wu, Q., Chiu, C. H., Fidler, I. J. Survival of cancer cells is maintained by EGFR independent of its kinase activity. Cancer Cell [Internet]. 2008 [cited 2016 Nov 2];13:385–93. http://www.sciencedirect.com/science/article/pii/S1535610808001207.
5. Parnian, J., Hoseindokht, M., Khademi, Z., & Moosavi, M. (2022). Calumenin knockdown, by intronic artificial microRNA, to improve expression efficiency of the recombinant human coagulation factor IX. Biotechnol Lett [Internet]. ; https://doi.org/10.1007/s10529-022-03249-8.
6. Satpathy, M., Mezencev, R., Wang, L., & McDonald, J. F. Targeted in vivo delivery of EGFR siRNA inhibits ovarian cancer growth and enhances drug sensitivity. Scientific Reports 2016 6:1 [Internet]. 2016 [cited 2023 Apr 28];6:1–9. https://www.nature.com/articles/srep36518.
7. Wan, X., Sun, R., Bao, Y., Zhang, C., Wu, Y., & Gong, Y. (2021). In vivo delivery of siRNAs targeting EGFR and BRD4 expression by peptide-modified redox responsive PEG-PEI nanoparticles for the treatment of triple-negative breast cancer. Mol Pharm [Internet]. [cited 2023 Apr 28];18:3990–8. https://pubmed.ncbi.nlm.nih.gov/34591491/.
8. Paul, A., Muralidharan, A., Biswas, A., Kamath, B. V., Joseph, A., & Alex, A. T. (2022). siRNA therapeutics and its challenges: Recent advances in effective delivery for cancer therapy. *OpenNano*, *7*, 100063.
9. Aslam, H., Shukrullah, S., Naz, M. Y., Fatima, H., Hussain, H., Ullah, S. Current and future perspectives of multifunctional magnetic nanoparticles based controlled drug delivery systems [Internet]. J Drug Deliv Sci Technol. 2022 [cited 2023 May 20]. https://www.sciencedirect.com/science/article/pii/S1773224721006262.
10. You, J., Wang, L., Zhao, Y., & Bao, W. A review of amino-functionalized magnetic nanoparticles for water treatment: Features and prospects. J Clean Prod [Internet]. 2021 [cited 2023 May 20];281. https://www.sciencedirect.com/science/article/pii/S0959652620347120.
11. Van de Walle, A., Perez, J. E., Abou-Hassan, A., Hémadi, M., Luciani, N., & Wilhelm, C. Magnetic nanoparticles in regenerative medicine: What of their fate and impact in stem cells? [Internet]. Mater Today Nano. 2020 [cited 2023 May 20]. https://www.sciencedirect.com/science/article/pii/S2588842020300134.
12. Gavilán, H., Avugadda, S. K., Fernández-Cabada, T., Soni, N., Cassani, M., Mai, B. T. Magnetic nanoparticles and clusters for magnetic hyperthermia: Optimizing their heat performance and developing combinatorial therapies to tackle cancer [Internet]. Chem Soc Rev. 2021 [cited 2023 May 20]. pp. 11614–67. https://pubs.rsc.org/en/content/articlehtml/2021/xx/d1cs00427a.
13. Kao, Y. T., Chen, Y. T., Fan, H. C., Tsai, T. C., Cheng, S. N., Lai, P. S. Novel coagulation factor viii gene therapy in a mouse model of hemophilia a by lipid-coated Fe_3o_4 nanoparticles. Biomedicines [Internet]. 2021 [cited 2023 May 20];9. https://www.mdpi.com/1250796.
14. Li, Y., & Zhang, H. (2019). Fe_3O_4-based nanotheranostics for magnetic resonance imaging-synergized multifunctional cancer management. *Nanomedicine: The Official Journal of the American Academy of Nanomedicine*, *14*, 1493–1512.
15. De Jong, W. H., & Borm, P. J. A. (2008). Drug delivery and nanoparticles: Applications and hazards. Int J Nanomedicine [Internet]. [cited 2023 May 5];3:133. http:///pmc/articles/PMC2527668/.
16. Raval, N., Maheshwari, R., Kalyane, D., Youngren-Ortiz, S. R., Chougule, M. B., & Tekade, R. K. Importance of physicochemical characterization of nanoparticles in pharmaceutical product development. Basic Fundamentals of Drug Delivery [Internet]. 2018 [cited 2023 May 20]. pp. 369–400. https://www.sciencedirect.com/science/article/pii/B9780128179093000108.

17. Angelopoulou, A., Kolokithas-Ntoukas, A., Fytas, C., & Avgoustakis, K. Folic acid-functionalized, condensed magnetic nanoparticles for targeted delivery of doxorubicin to tumor cancer cells overexpressing the folate receptor. ACS Omega [Internet]. 2019 [cited 2023 May 20];4:22214–27. https://doi.org/10.1021/acsomega.9b03594.
18. Bu, L. L., Rao, L., Yu, G. T., Chen, L., Deng, W. W., Liu, J. F. (2019). Cancer stem cell-platelet hybrid membrane-coated magnetic nanoparticles for enhanced photothermal therapy of head and neck squamous cell carcinoma. Adv Funct Mater [Internet]. [cited 2023 May 20];29. https://onlinelibrary.wiley.com/doi/abs/https://doi.org/10.1002/adfm.201807733.
19. Parnian, J., Ma'mani, L., Bakhtiari, M. R., & Safavi, M. (2022). Overcoming the non-kinetic activity of EGFR1 using multi-functionalized mesoporous silica nanocarrier for in vitro delivery of siRNA. Sci Rep [Internet]. [cited 2022 Nov 7];12:1–17. https://www.nature.com/articles/s41598-022-21601-w.
20. Salekdeh, P. R., Ma'mani, L., Tavakkoly-Bazzaz, J., Mousavi, H., Modarressi, M. H., & Salekdeh, G. H. (2021). Bi-functionalized aminoguanidine-PEGylated periodic mesoporous organosilica nanoparticles: A promising nanocarrier for delivery of Cas9-sgRNA ribonucleoproteine. *J Nanobiotechnology*. ;19.
21. Cun, D., Jensen, D. K., Maltesen, M. J., Bunker, M., Whiteside, P., Scurr, D. (2011). High loading efficiency and sustained release of siRNA encapsulated in PLGA nanoparticles: Quality by design optimization and characterization. European Journal of Pharmaceutics and Biopharmaceutics [Internet]. [cited 2021 Sep 25];77:26–35. https://www.sciencedirect.com/science/article/pii/S0939641110002973.
22. Liu, W., & Tsou, C. L. (1987). Activity change during unfolding of bovine pancreatic ribonuclease A in guanidine. Biochimica et Biophysica Acta (BBA)/Protein Structure and Molecular [Internet]. [cited 2022 Jan 8];916:455–64. https://www.sciencedirect.com/science/article/pii/0167483887901920.
23. Haghighat, N., Abdolmaleki, P., Parnian, J., & Behmanesh, M. The expression of pluripotency and neuronal differentiation markers under the influence of electromagnetic field and nitric oxide. Molecular and Cellular Neuroscience [Internet]. 2017 [cited 2020 Dec 13];85:19–28. https://www.sciencedirect.com/science/article/pii/S1044743117302129.
24. Hossen, S., Hossain, M. K., Basher, M. K., Mia, M. N. H., Rahman, M. T., & Uddin, M. J. (2019). Smart nanocarrier-based drug delivery systems for cancer therapy and toxicity studies: A review. J Adv Res. Elsevier; pp. 1–18.
25. Poonia, N., Lather, V., & Pandita, D. (2018). Mesoporous silica nanoparticles: A smart nanosystem for management of breast cancer. Drug Discov Today. Elsevier; pp. 315–32.
26. Bivas-Benita, M., Romeijn, S., Junginger, H. E., & Borchard, G. (2004). PLGA-PEI nanoparticles for gene delivery to pulmonary epithelium. *European Journal of Pharmaceutics and Biopharmaceutics, 58*, 1–6.
27. Boussif, O., LezoualC'H, F., Zanta, M. A., Mergny, M. D., Scherman, D., & Demeneix, B. (1995). A versatile vector for gene and oligonucleotide transfer into cells in culture and in vivo: Polyethylenimine. *Proc Natl Acad Sci U S A, 92*, 7297–301.
28. Godbey, W. T., Wu, K. K., Hirasaki, G. J., & Mikos, A. G. (1999). Improved packing of poly(ethylenimine)/DNA complexes increases transfection efficiency. *Gene Ther, 6*, 1380–8.
29. Kircheis, R., Wightman, L., & Wagner, E. Design and gene delivery activity of modified polyethylenimines [Internet]. Adv Drug Deliv Rev. 2001 [cited 2020 Dec 13]. pp. 341–58. https://www.sciencedirect.com/science/article/pii/S0169409X01002022.
30. Yamazaki, Y., Nango, M., Matsuura, M., Hasegawa, Y., Hasegawa, M., & Oku, N. (2000). Polycation liposomes, a novel nonviral gene transfer system, constructed from cetylated polyethylenimine. *Gene Ther, 7*, 1148–55.
31. Watermann, A., & Brieger, J. Mesoporous silica nanoparticles as drug delivery vehicles in cancer [Internet]. Nanomaterials. Multidisciplinary Digital Publishing Institute; 2017 [cited 2021 Sep 14]. p. 189. https://www.mdpi.com/2079-4991/7/7/189/htm.
32. Lu, J., Liong, M., & Zink, J. (2007). Mesoporous silica nanoparticles as a delivery system for hydrophobic anticancer drugs. Small [Internet]. [cited 2017 Feb 16];3:1341–6. http://onlinelibrary.wiley.com/doi/https://doi.org/10.1002/smll.200700005/full.
33. Arsianti, M., Lim, M., Marquis, C. P., & Amal, R. (2010). Assembly of polyethylenimine-based magnetic iron oxide vectors: Insights into gene delivery. *Langmuir*, *26*, 7314–7326.
34. Namgung, R., Singha, K., Yu, M. K., Jon, S., Kim, Y. S., Ahn, Y., et al. (2010). Hybrid superparamagnetic iron oxide nanoparticle-branched polyethylenimine magnetoplexes for gene transfection of vascular endothelial cells. *Biomaterials*, *31*, 4204–4213.
35. Quaglia, F., Ostacolo, L., Mazzaglia, A., Villari, V., Zaccaria, D., & Sciortino, M. T. (2009). The intracellular effects of non-ionic amphiphilic cyclodextrin nanoparticles in the delivery of anticancer drugs. Biomaterials [Internet]. [cited 2021 Sep 25];30:374–82. https://www.sciencedirect.com/science/article/pii/S0142961208007011.
36. Acharya, G., Shin, C. S., Vedantham, K., McDermott, M., Rish, T., Hansen, K. A study of drug release from homogeneous PLGA microstructures. Journal of Controlled Release [Internet]. 2010 [cited 2021 Sep 25];146:201–6. https://www.sciencedirect.com/science/article/pii/S016836591000249X.
37. Slowing, I. I., Vivero-Escoto, J. L., Wu, C. W., & Lin, V. S. Y. Mesoporous silica nanoparticles as controlled release drug delivery and gene transfection carriers [Internet]. Adv Drug Deliv Rev. 2008 [cited 2020 Dec 13]. pp. 1278–88. https://www.sciencedirect.com/science/article/pii/S0169409X08000951.
38. Neuhaus, B., Tosun, B., Rotan, O., Frede, A., Westendorf, A. M., & Epple, M. (2016). Nanoparticles as transfection agents: A comprehensive study with ten different cell lines. RSC Adv [Internet]. [cited 2021 Sep 14];6:18102–12. https://pubs.rsc.org/en/content/articlehtml/2016/ra/c5ra25333k.
39. Horibe, T., Torisawa, A., Akiyoshi, R., Hatta-Ohashi, Y., Suzuki, H., & Kawakami, K. (2014). Transfection efficiency of normal and cancer cell lines and monitoring of promoter activity by single-cell bioluminescence imaging. *Luminescence*, *29*, 96–100.
40. Müller, K., Kessel, E., Klein, P. M., Höhn, M., & Wagner, E. (2016). Post-PEGylation of siRNA lipo-oligoamino amide polyplexes using tetra-glutamylated folic acid as ligand for receptor-targeted delivery. *Molecular Pharmaceutics*, *13*, 2332–2345.
41. Gabizon, A., Shmeeda, H., Horowitz, A. T., & Zalipsky, S. (2004). Tumor cell targeting of liposome-entrapped drugs with phospholipid-anchored folic acid-PEG conjugates. *Advanced Drug Delivery Reviews*, *56*, 1177–1192.
42. Zwicke, G. L., Mansoori, G. A., & Jeffery, C. J. (2012). Targeting of Cancer Nanotherapeutics. *Nano Rev*, *1*, 1–11.
43. Abe, S., Kida, I., Esaki, M., Akasaka, T., Uo, M., Hosono, T., Sato, Y., Jeyadevan, B., Kuboki, Y., Morita, M., & Tohji, K. (2009). Biodistribution imaging of magnetic particles in mice: X-ray scanning analytical microscopy and magnetic resonance imaging. *Biomedical Materials and Engineering*, *19*(2–3), 213–220.